

1 **Geotechnical characterization of the estuarine deltaic deposits in the Guayaquil**
2 **City through in situ and laboratory tests.**

3 Bosco Intriago^a, Hernán Bazurto^a, Davide Besenon^a, Xavier Vera-Grunauer^b, Sara Amoroso^{c, d}

4 ^a*Facultad de Ingeniería en Ciencias de la Tierra, Escuela Superior Politécnica del Litoral, Campus Gustavo Galindo*
5 *Km 30.5 Vía Perimetral, P.O. Box 09-01-5863, Guayaquil, Ecuador*

6 ^b*Geoestudios S.A., Cda. Kennedy Norte, Calle José Assaf Mz 704, V 3, Guayaquil 090512, Ecuador*

7 ^c*Department of Engineering and Geology, University of Chieti-Pescara, Viale Pindaro 42, 65129 Pescara, Italy*

8 ^d*Istituto Nazionale di Geofisica e Vulcanologia, Italy*

9 **HIGHLIGHTS**

10 Geotechnical and geophysical characterization of a test site in Ecuador

11 Comparative analyses of the geotechnical and geophysical parameters for soft clays with diatoms

12 Shear wave velocity predictive equations using different in situ tests

13 Stiffness decay curves estimated using the seismic dilatometer test

14 **ABSTRACT**

15 Guayaquil city is located on the West margin of the Guayas River along the Pacific coast of South
16 America. According to research and zoning from previous studies a large area of the city sits on
17 estuarine deltaic deposits which consist of weak and highly compressible clays with diatoms. The
18 nature of these soft clays may determine difficulties in the use of some methods or equations, and
19 consequently in the reliability of the obtained interpretation of the results. This paper focuses on
20 evaluating the most recommended methods and equations for this type of deposits. In this respect,
21 a detailed geotechnical and geophysical characterization of the study area has been carried out.
22 Borehole logs, standard penetration tests (SPT), piezocone tests (CPTu), seismic dilatometer test
23 (SDMT), non-invasive geophysical survey and laboratory tests were performed and compared to
24 analyze static and dynamic geotechnical parameters of these soft clays, resulted sensitive to the
25 presence of diatoms.

26 *Keywords:* seismic dilatometer test, piezocone test, soft clays, diatoms, estuarine deltaic deposits,
27 geotechnical characterization.

28 **1. Introduction**

29 In the last decades, Guayaquil soils have been widely studied because of an increasing urban process
30 that the Ecuadorian city has experienced. Nevertheless, limited information is available in the
31 literature about estimation of geotechnical parameters related to this area.

32 The estuarine zone of the Guayas River deposits is highly heterogeneous. The soil stratigraphy
33 consists of very soft, weak, and highly compressible sediment over hard rocks of Piñon and Cayo
34 Fm. (Vera-Grunauer, 2014). These soils, once analyzed microscopically, show in their matrix clay
35 minerals of heterogeneous composition. One of these components are diatoms. Diatoms are single
36 shelled plants that grow in fresh or salty water rich in dissolved silica, consuming the dissolved
37 silica to build up their skeletons (Treguer et al., 1995; Antonides, 1998). The chemical composition
38 of diatoms and their porous microstructure affect clay behavior, because the diatom skeletons or
39 frustules contain a large number of voids, approximately between 60 and 70% according to Losic
40 et al. (2007). These spaces allow great absorption of water which leads to a possible alteration of
41 the soil properties. Díaz-Rodríguez et al. (2013) also determined that microfossils in significant
42 quantities influence the soil behavior, especially with reference to compressibility parameters.

43 Caicedo et al. (2018) established that for Bogotá soils, diatoms increase the plasticity index (PI),
44 compromising the use of the Unified Soil Classification System (USCS, ASTM, 2011). Shiwakoti
45 et al. (2002) reached a similar consideration indicating that the Atterberg limits have a significant
46 increase due to the presence of diatoms. Moreover, as long as the concentration of diatoms increases,
47 the coefficients of compressibility and permeability increase. Due to the rough surface and
48 interlocking shape of the minerals, the effective friction angle and shear strength rise too.

49 Vera-Grunauer (2014) developed several studies on Guayaquil clays with diatoms, confirming the
50 above mentioned evidence. Moreover, Torres et al. (2018) studied the space-temporal variability of
51 phytoplankton and oceanographic variables in the Gulf of Guayaquil between 2013 and 2015,

52 finding 166 species of phytoplankton, 32 of which were diatoms and whose distribution depends on
53 the depth, being more abundant in the first 20 m. This considerable presence of diatoms in Guayaquil
54 deposits assumes importance considering that the majority of the methods or geotechnical
55 correlations are calibrated on datasets that do not consider the diatom content in soft clays. A proper
56 characterization of soil parameters requires an integrated approach whereby the geophysical
57 method, in situ and laboratory tests are used. However, data obtained from in situ tests depend on
58 many factors including stress history, grain size, minerals, composition and packing of the particles.
59 Consequently, a generalized correlation, consistent for some soil types, not necessarily fit well for
60 other geomaterials (Mayne, 2006).

61 In Ecuador, the standard penetration test (SPT) is overused for the geotechnical design. This practice
62 is attributed to its widespread use worldwide during the last decades, which has led to the collection
63 of a considerable number of data and correlations, considering the limited cost of execution during
64 the cores, the usual availability of the SPT equipment, and the easy execution. However, its use
65 should not be generalized in all soils, especially in soft clays. The results are difficult to interpret in
66 cohesive deposits and, consequently, not conclusive due to the low number of blows. Besides, the
67 samples obtained are highly altered, and therefore they are not representative of the in situ conditions
68 (Mayne et al., 2009). In this respect, it is advisable to use other in situ tests, such as the piezocone
69 test (CPTu) and the seismic dilatometer test (SDMT), to better capture the undrained and drained
70 behavior of cohesive and incoherent soils, respectively. Among the main advantages of in situ tests,
71 there are the ease of execution, the economic savings between taking the sample and its analysis in
72 the laboratory, the reduction in the alteration of the soil by evaluating its natural state, and the
73 possibility of investigating in greater detail the spatial variability of the subsoil according to
74 Devincenzi et al. (2007). This paper aims to compare laboratory test data and in situ test results at a
75 soft clay site in Guayaquil to evaluate and provide the most appropriate correlations to capture the
76 behavior of these estuarine deposits.

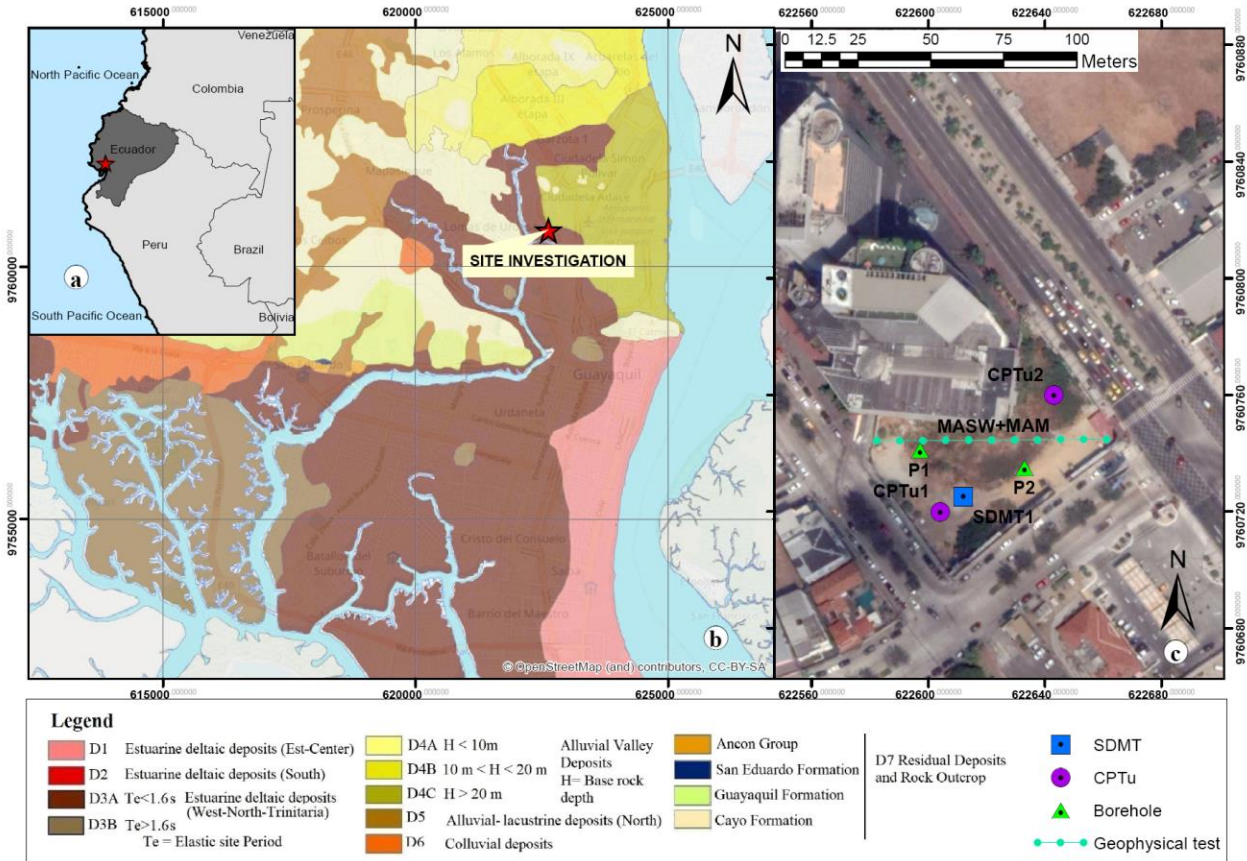
77 **2. Site investigation**

78 **2.1. Geological setting**

79 Ecuador is considered a country with high seismic risk, being located on an active subduction
80 tectonic margin with direction N80°E (Benítez, 1995; Egüez et al., 2003), where the Nazca plate
81 collides and subducts with the Continental segment formed by the Northern Andean block and the
82 Southern American plate (Chunga et al., 2019).

83 The study area of this research, Guayaquil city, is located in the Ecuadorian coastal region. This
84 area presents different geological formations, where the three main representative geological units
85 are known as the formations of Guayaquil, Cayo, and Piñon (Benítez et al., 2005). These
86 geomorphological features of Guayaquil supports the convergence of three geological macro-
87 domains: (1) alluvial plain of the Daule and Babahoyo rivers; (2) Chongón-Colonche Cordillera
88 hills; (3) estuarine deltaic complex of the Guayas River.

89 Vera-Grunauer (2014) developed a seismic microzonation map of Guayaquil, classifying the city
90 into seven lithological units. The study area, namely Murano, is located in Kennedy Norte sector
91 (North-East of the city), along two estuarine branches and characterized by soft unconsolidated
92 sediments. According to Vera-Grunauer (2014), the site corresponds to the lithological unit D3. This
93 zone is defined as Holocene estuarine deltaic deposits, in which sub-classification D3A and D3B
94 correspond to initial elastic periods $T_e < 1.6$ s, $T_e > 1.6$ s, respectively (Figs. 1a and 1b). Kennedy
95 Norte zone presents different lithological features that can amplify or attenuate differently seismic
96 waves into the ground during an earthquake (Chunga et al., 2005). For this reason, it is important to
97 establish geotechnical parameters for a specific site.



98

99

Fig. 1. Location of the test site (a) and geological map of the study area (b). Location of the site investigations at the Murano site (c).

100

101

2.2. Description of the Site Campaign

102

Multiple geotechnical and geophysical surveys were carried out at the site to reconstruct a more accurate subsoil characterization at Murano site. The location of the boreholes and the other investigations is reported in Fig. 1c. The investigations included n. 2 boreholes (P-1 and P-2) at depths of 46 and 45 m respectively, with the execution of SPTs and the retrieval of disturbed samples for soil classification (i.e. sieve analyses and Atterberg limits) approximately each meter of depth. Moreover, n. 3 undisturbed samples were collected at 3.70, 6.60 and 7.50 m of depth to perform oedometric and unconfined compression tests. In situ tests included n. 2 piezocone tests, namely CPTu1 and CPTu2, at 41 and 30 m of depth respectively, and n. 1 seismic dilatometer (SDMT1) test at 31 m of depth. Due to the irregular topography of the area for the presence of a non-penetrable fill, in situ tests needed a predrilled hole up to 2 m depth. Dissipation tests were performed at specific depths for both CPTu and SDMT tests (see Table 1 for details). With reference to geophysical

112

113 measurements a multichannel analysis of surface waves (MASW) survey was performed with a
 114 microtremor array measurement (MAM) test for a total length of 80.5 m.

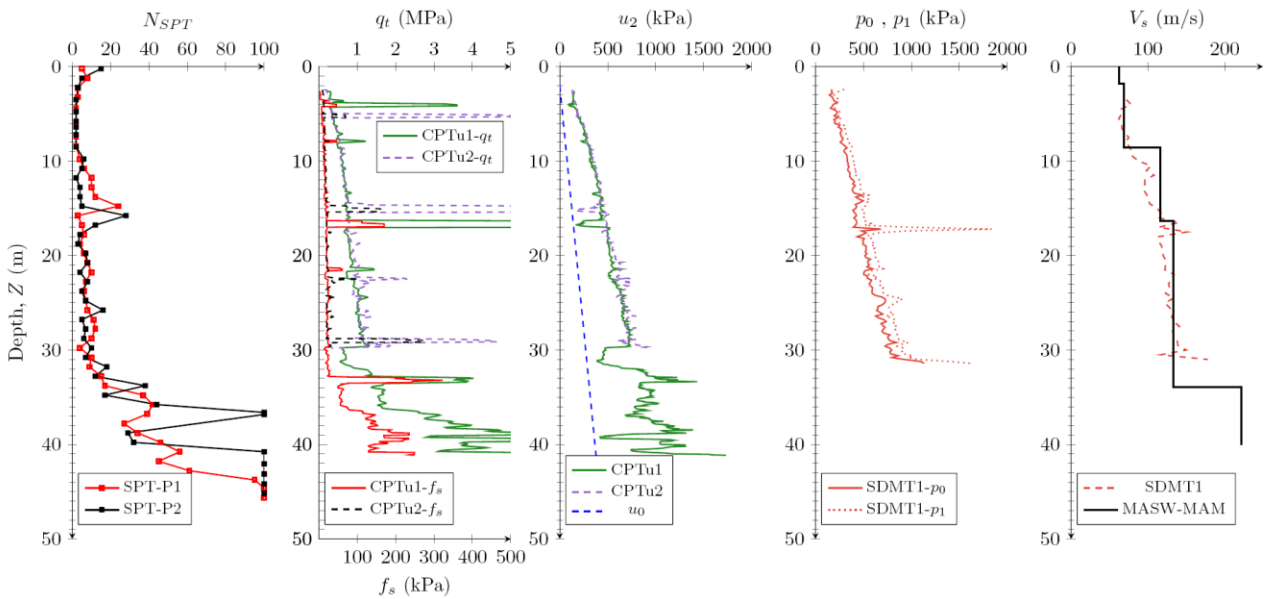
115 **Table 1.** Summary of the field investigations performed at Murano site.

Field test	Depth* (m)	Dissipation test depth (m)	Disturbed samples	Undisturbed samples	SPT per borehole	GWT depth (m)	Test date
P1	46.00	-	45	1	45	1.80	14/11/2018
P2	45.00	-	45	2	45	2.00	08/11/2018
CPTu1	41.00	10.60; 13.45	-	-	-	2.05	12/11/2018
CPTu2	30.00	8.00; 12.00	-	-	-	1.82	09/11/2018
MASW+MAM	80.50	-	-	-	-	-	-
SDMT1	31.40	8.00	-	-	-	3.00	05/08/2018

116 *For MASW+MAM this refers to length.

117 2.3 Direct Measurements

118 Fig. 2 summarizes the results of the direct measurements obtained from the in situ geotechnical and
 119 geophysical investigations. In particular for SPT the blow counts (N_{SPT}), necessary to penetrate the
 120 sampler 300 mm into the ground, after advanced first penetration of 150 mm, are reported. For
 121 CPTu, the readings of the corrected cone resistance (q_t), sleeve friction (f_s), and pore water pressure
 122 (u_2) are plotted. For the flat dilatometer (DMT) test, introduced by Marchetti (1980), the profiles of
 123 the two corrected pressure readings, namely p_0 (1st reading) and p_1 (2nd reading), are illustrated in
 124 Fig. 2. The low N_{SPT} and q_t measurements and the high f_s and u_2 values in the upper 30 m of depth,
 125 together with the proximity of p_0 and p_1 pressures depth by depths, agree to preliminarily identify
 126 the profile of a soft and clayey soil. Moreover, for DMT one measurement for the 3rd corrected
 127 pressure reading (p_2) is available and equal to 135 kPa in a thin sandy layer located at 17 m of depth.
 128 According to Marchetti et al. (2001), p_2 values are generally used to estimate the hydrostatic water
 129 level in incoherent deposits. Therefore, the ground water level (GWT) can be estimated at 3 m of
 130 depth at the DMT test site. CPTu test can be also used to estimate the GWT through u_2 ; in this case
 131 GWT is at about 2 m for CPTu1 and 1.82 m for CPTu2. For boreholes P1 and P2, GWT was
 132 measured at 1.8 and 2 meters of depth respectively. CPTu tests and boreholes were performed
 133 roughly in the same wet period (see Table 1), which justifies the good agreement between GWT
 134 results. On the contrary, SDMT1 was performed in the Ecuadorian dry season, explaining the GWT
 135 variation due to seasonal fluctuations.



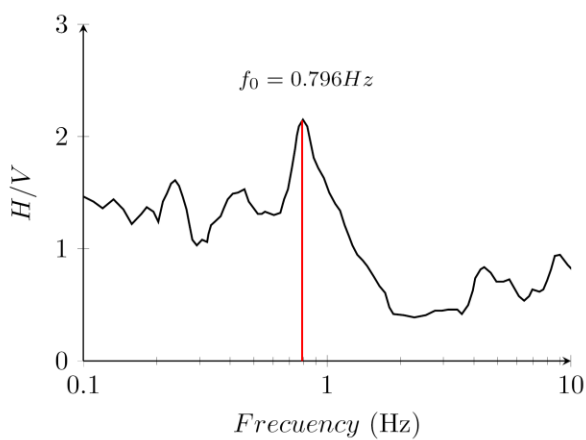
136
 137 **Fig. 2.** Measured parameters for geotechnical and geophysical tests at Murano site: SPT blow counts
 138 (N_{SPT}), corrected cone resistance (q_t), sleeve friction (f_s), pore water pressure (u_2), corrected DMT
 139 readings (p_0 , p_1), shear wave velocity (V_s).

140 Finally, Fig. 2 plots the shear wave velocity (V_s) data carried out from the SDMT test (Marchetti et
 141 al., 2008) and from the combined interpretation of the dispersion curves related to the active MASW
 142 survey and the passive MAM measurements (Park et al., 2007). The two independent V_s profiles
 143 highlight a good agreement between the geophysical and geotechnical methods, thus strengthening
 144 the reliability of the acquisitions at the test site.

145 The passive measurements also provide the ambient noise vibrations, in terms of Horizontal to
 146 Vertical, namely H/V, curves, as shown in Fig. 3. The graph detects a peak frequency (f_0) at 0.796
 147 Hz, that corresponds to an elastic period (T_e) of 1.256 s. This value correctly matches with the
 148 seismic microzonation study (Vera-Grunauer, 2014) that identifies the Murano area as D3A zone,
 149 namely estuarine deltaic deposits with $T_e < 1.6$ s.

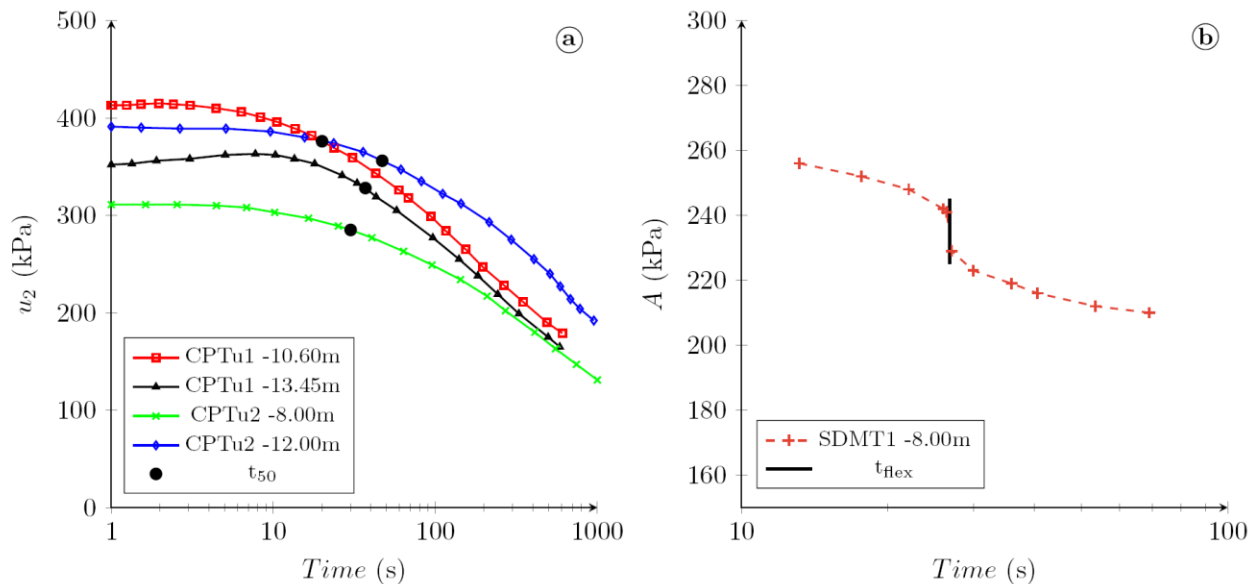
150 Other direct measurements obtained at the site are related to dissipation tests from CPTu and DMT
 151 tests, as for the coefficient of consolidation in horizontal direction (c_h) (Robertson et al., 1992;
 152 Marchetti and Totani, 1989). Fig. 4a shows the results of the CPTu pore water pressure (u_2) with
 153 the time (t) together with the points corresponding to the measured time for the 50% of the
 154 dissipation (t_{50}), while Fig. 4b illustrates the profile of the non-corrected 1st DMT reading (A) with

155 the time (t) in combination with the contraflexure point of the curve (t_{flex}). c_h values obtained in the
 156 layer at 8.00 m depth by CPTu and DMT is in good agreement and is equal to an average of $3 \cdot 10^{-5}$
 157 m^2/sec , while c_h provides values between $2 \cdot 10^{-5}$ and $5 \cdot 10^{-5} m^2/sec$ in the bottom layer between 10.60
 158 and 13.45 m of depth.
 159 All together the SPT, CPTu, SDMT and MASW+MAM direct measurements preliminarily agree to
 160 identify a homogeneous site. However, the data interpretation that will follow in the next paragraphs
 161 will provide further details.



162

163 **Fig. 3.** H/V curves from passive measurements.



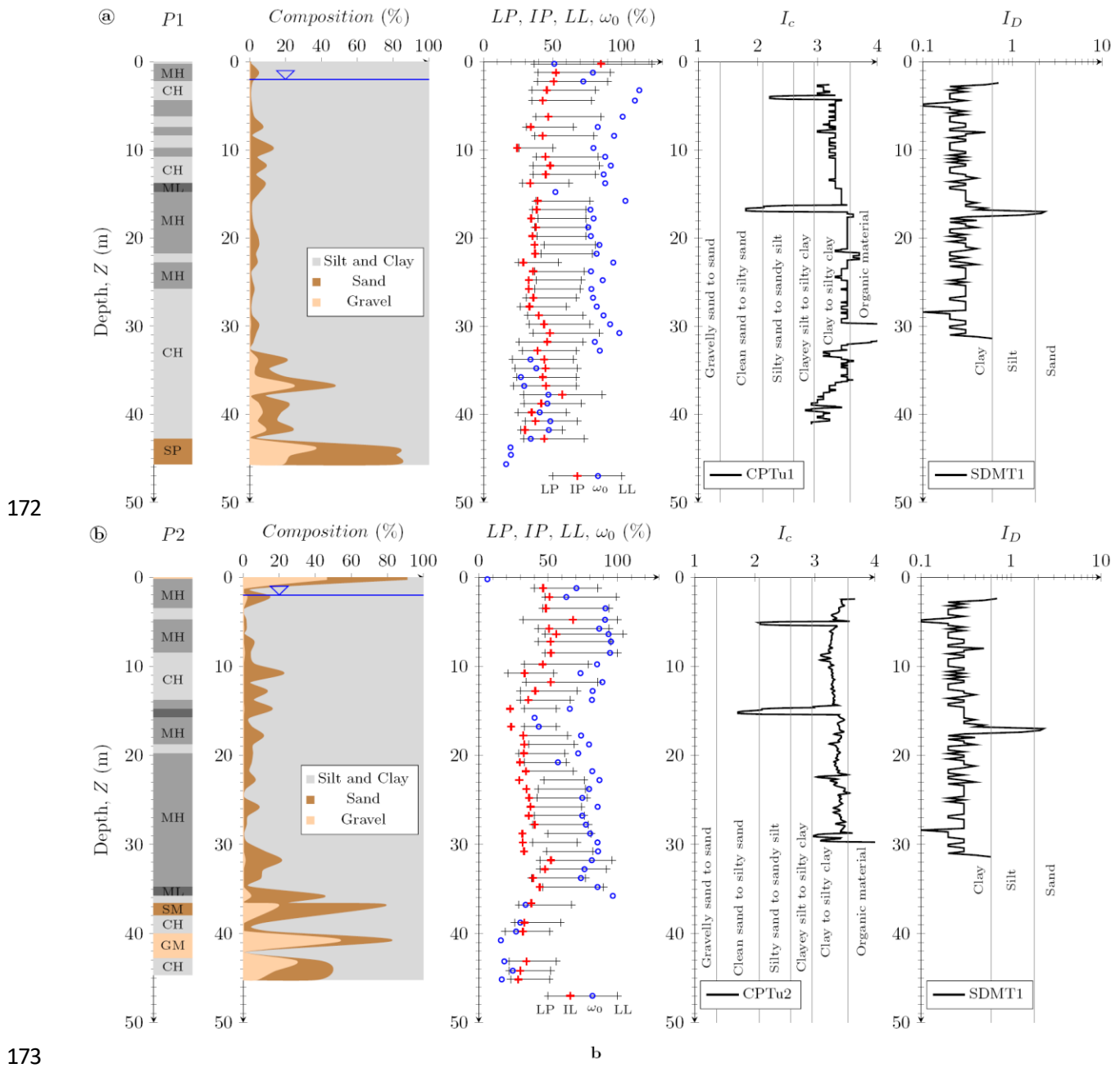
164

165 **Fig. 4.** Dissipation tests from CPTu (a) and DMT (b) tests.

166 **3. Geotechnical characterization of the test site using in situ and laboratory tests**

167 **3.1. Soil classification**

168 Laboratory and in situ testing were analyzed to obtain a detailed soil classification. Fig. 5 shows the
 169 borehole log using USCS soil classification, the soil composition, the Atterberg limits (liquid limit
 170 LL, plastic limit LP), the plasticity index (PI) and the water content (w), the CPT soil behavior type
 171 index (I_c) and the DMT material index (I_D).



174 **Fig. 5.** Soil classification using USCS method, CPTu and DMT interpretations, soil composition
 175 and basic properties for boreholes P1 (a) and P2 (b).

176 The soil stratigraphy is apparently quite uniform up to approximately 33-37 m, showing mainly
 177 clays with high plasticity (mean plasticity index $PI > 40\%$) and liquid limit (mean liquid limit $LL >$

178 70%). In particular, from 0 to 15 m the predominance of silts and clays soil is observed,
179 characterized by an average PI of 46% and w of about 86%. The fines continue to predominate from
180 15 to 30-37 m, but the percent of sand starts to increase and the IP and w values decrease staying in
181 a range of 30-50% and 70-90%, respectively. Below 30-37 m of depth, the percentage of sand
182 continues to increase up to 60% and also a relevant presence of gravel (37-54%) is encountered.
183 Consequently, Atterberg limits and water content values decrease.

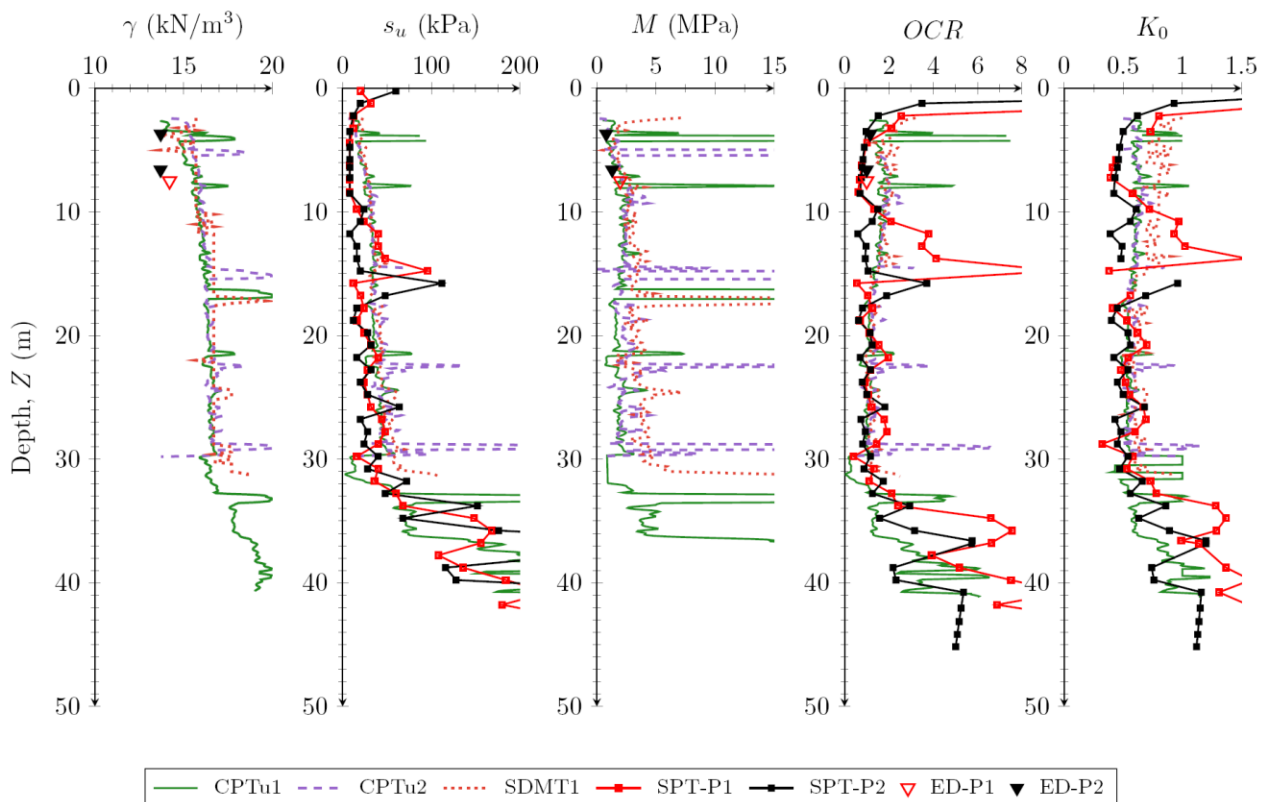
184 I_c and I_D profiles, estimated using Robertson and Cabal (2015) and Marchetti et al. (2001)
185 respectively, are in broad agreement with the soil stratigraphy obtained from the boreholes and the
186 lab testing, since in situ tests detect on average a clay layer up to 40 m depth with a thin sandy sand
187 lens between 15 and 17 m depth. However, there is not a perfect correspondence between the CPT-
188 DMT geotechnical description and the grading curves (i.e. soil composition percent), since both I_c
189 and I_D are parameters related to the mechanical soil response and not strictly to the grain size of the
190 soil deposits (e.g. Boncio et al., 2020). The integrated information of gradations and index properties
191 may find better agreement with I_c and I_D values. For example, correspondence to low-plastic
192 deposits by P2 (Fig. 5b) is noticed for the silty sands detected by CPTu2 at about 15 m.

193 Finally, it can be observed that for most of the soil samples within the upper 30-37 m depth w is
194 generally higher than 70%, recording also values bigger than 100%. Particularly, highest PI, LL, LP
195 and w values are concentrated in the upper 15 m depth. This information is in relevant agreement
196 with Vera-Grunauer (2014) who performed scanning electron micrographs for soil samples taken at
197 sites close to the studied area. Vera-Grunauer (2014) observed that the microporous structure of
198 diatoms has a diameter less than 0.5 μm which generates a large specific surface area and allows the
199 absorption of a large amount of water. Moreover, Vera-Grunauer (2014) developed a graph in which
200 it is evidenced that for the lithological zone D3, where the study area is located, the relationship
201 between w and LL varies mainly between 0.8 to 1.2, presenting a greater tendency to values close
202 to 1. This information is consistent with the present research where it can be verified that the water

203 content is greater or very close to the liquid limit, as shown in Fig. 5. Therefore, the greater water
 204 content is because of water absorption caused by the diatom pores as mentioned above.

205 3.2. Strength and compressibility

206 The soil total unit weight (γ) is an important parameter because it indirectly shows an idea of the
 207 field state of stress of a soil at a desired depth (Rodríguez et al., 2015). The total unit weight value
 208 depends on the water content located in the voids as well as the density or weight of the mineral
 209 grains. Recommended values of total unit weight were proposed by Look (2007) for cohesive soils,
 210 from soft organic with $\gamma \approx 14 \text{ kN/m}^3$, to soft non organic with $\gamma \approx 16 \text{ kN/m}^3$ and to stiff to hard with
 211 γ between 18 to 20 kN/m^3 . Laboratory tests on undisturbed samples (ED-P1, ED-P2, Fig. 6) carried
 212 out at the Murano site show $\gamma \approx 14\text{-}16\text{ kN/m}^3$. These low values are in agreement with typical
 213 behavior of soft soils and are probably related also the presence of siliceous diatoms randomly
 214 distributed in the soil mass (Vera-Grunauer, 2014).



215

216 **Fig. 6.** Geotechnical parameters estimated from laboratory and in situ tests.

217 On the contrary, the γ profiles obtained from CPTu and DMT interpretations, according to
 218 Robertson and Cabal (2015) and Marchetti and Crapps (1981) charts respectively, provide higher
 219 unit weight values in correspondence of coarser layers. Simultaneously, a general increase of γ is
 220 detectable with the depth into the homogeneous clay, due to the increase of effective vertical stress
 221 (σ'_{v0}). In general, soil unit weights are best obtained by relatively undisturbed samples, while the
 222 main scope of CPTu and DMT charts is not an accurate estimation of γ , but the possibility of
 223 constructing an approximate σ'_{v0} profile, needed in the elaboration of the in situ tests (Robertson
 224 and Cabal, 2015; Marchetti et al., 2001).

225 Undrained shear strength (s_u) coupled with total stress analysis is often used to examine the failure
 226 state of geotechnical structures under undrained conditions in Guayaquil City (Vera-Grunauer,
 227 2014). For SPT, Brown and Hettiarachchi (2008) recommend a correlation based on the energy
 228 corrected SPT blow count (N_{60}) values:

$$s_u = 4.1 \cdot N_{60} \quad (1)$$

229 with

$$N_{60} = C_E \cdot N_{SPT} \quad (2)$$

230 C_E is the energy correction factor, equal to 1.02-1.04, obtained from the measurements of the
 231 measured hammer energy at the Murano site.

232 A theoretical solution for CPTu test interpretation is in the form:

$$s_u = (q_t - \sigma_{v0}) / N_{kt} \quad (3)$$

233 where σ_{v0} is the total vertical stress and N_{kt} is a factor that varies from 10 to 18, with 14 as an average
 234 (Robertson, 2010).

235 Finally, for DMT test s_u is obtained by the following equation (Marchetti, 1980):

$$s_u = 0.22 \cdot \sigma'_{v0} (0.5 \cdot K_D)^{1.25} \quad (4)$$

236 with

$$K_D = (p_0 - u_0) / \sigma'_{v0} \quad (5)$$

237 where p_0 is the corrected 1st reading and u_0 is the hydrostatic pore water pressure. K_D is the horizontal
238 stress index that provides the basis for several soil parameter correlations, coming out as the key
239 result of the dilatometer test. In this respect, K_D can be regarded as an amplified in situ earth pressure
240 coefficient (K_0) because $(p_0 - u_0)$ is an “amplified” horizontal effective stress (σ'_{h0}), due to
241 penetration. In genuinely NC clays (no aging, structure, cementation) the value of K_D is
242 approximately equal to 2, and this justifies that the K_D profile is similar in shape to the
243 overconsolidation ratio (OCR) profile, hence generally helpful for “understanding” the soil deposit
244 and its stress history (Marchetti, 1980; Jamiolkowski et al., 1988).

245 For s_u estimations CPTu and DMT present a satisfactory agreement, while SPT provides lower
246 values within the upper 20 m depth, moving closer to DMT and CPTu prediction at greater depth.
247 This is related to the fact that SPT may not capture the effect produced by diatoms and cementation
248 in clays due to the natural confinement and microstructure. SPT evaluation is susceptible to
249 distortion produced by the incorrect data processing and the calibration for the test execution.

250 Penetration test results are most commonly used to estimate the settlement behavior of the soils,
251 using the constrained modulus (M), that depend on the stress state, soil type, and degree of
252 preconsolidation. These dependencies are incorporated into CPT and DMT empirical correlations
253 since M from CPT (Robertson, 2009) is related to the soil behavior type index (I_c) and to the in situ
254 vertical stress, and M from DMT (Marchetti, 1980) is a function of the material index (I_D), of the
255 horizontal stress index (K_D) and of the dilatometer modulus (E_D , i.e. the elastic modulus of the
256 horizontal load test performed by the DMT membrane with 60 mm diameter and the 1.1 mm
257 displacement). The results evidence a correspondence between the samples evaluated by oedometer
258 test and in situ CPT and DMT tests within the upper 7 m depth, providing $M \approx 0.5\text{-}2.03$ MPa. CPT
259 and DMT predictions are still in reasonable agreement between 7 and 15 m depth ($M \approx 2.5$ MPa)
260 while at greater depths, DMT always provides higher values compared to CPT. According to the
261 numerous case histories available in the literature (e.g. Monaco et al. 2006, 2014; Schmertmann,
262 1986, 1988; Mayne, 2005; Berisavljevic 2017) DMT usually provides a good agreement between

263 measured and DMT-predicted settlements thanks to the high reliability of the DMT constrained
264 modulus M that is a working strain modulus. M by DMT is therefore associated with an intermediate
265 strain level, more appropriate for the settlement calculations. In contrast, penetration tests, like CPT,
266 working at higher strains due to the considerable distortion induced by the CPT conical tip, produce
267 a less reliable M estimation (Baligh and Scott, 1975; Mayne, 2001).

268 For evaluating the overconsolidation, the abovementioned strong dependence between K_D and stress
269 history in uncemented NC clay allowed the development of the following equation (Marchetti,
270 1980):

$$\text{OCR} = (0.5 \cdot K_D)^{1.56} \quad (8)$$

271 Later, Kulhawy and Mayne (1990), Mayne and Liao (2004) and Mayne (2016) noticed that the OCR
272 in CPT tests significantly influences the normalized values of the q_t , suggesting to use the following
273 formula in the analysis of fine-grained soils:

$$\text{OCR} = 0.3 \cdot (q_t - \sigma_{v0}) / \sigma'_{v0} \quad (9)$$

274 For SPT analysis, OCR was estimated using SHANSEP approach and site parameters S and m ,
275 proposed by Vera-Grunauer (2014):

$$s_u / \sigma'_{v0} = S \cdot (\text{OCR})^m \quad (10)$$

276 The values of S and m can be assumed equal to 0.22 and 0.75, respectively, for D3 estuarine deltaic
277 zone of Guayaquil, while s_u was obtained using Eq. (1). Fig. 6 shows OCR values from in situ and
278 oedometer tests. CPT and DMT are in good agreement for the entire profile, estimating $\text{OCR} \approx 2$
279 within the upper 15 m and a more defined NC behavior ($\text{OCR} \approx 1$) approximately between 15 and
280 30 m. On the contrary, oedometric tests underestimate OCR up to 15 m depth. This may be due to
281 the difficulties to retrieve high quality samples on soft clay soils which prevents to preserve soil
282 structure (e.g. Berisavljević et al., 2014).

283 CPT and SPT tests also provide a rough estimate of the in situ earth pressure coefficient (K_0) for
284 low plastic fine-grained soils, using the OCR values estimated by each own test (Kullhawy and
285 Mayne, 1990):

$$K_0=0.5 \cdot OCR^{0.5} \quad (11)$$

286 On the contrary DMT provide a reliable K_0 correlation in clay obtained experimentally by Marchetti
287 (1980) and theoretically by Yu (2004):

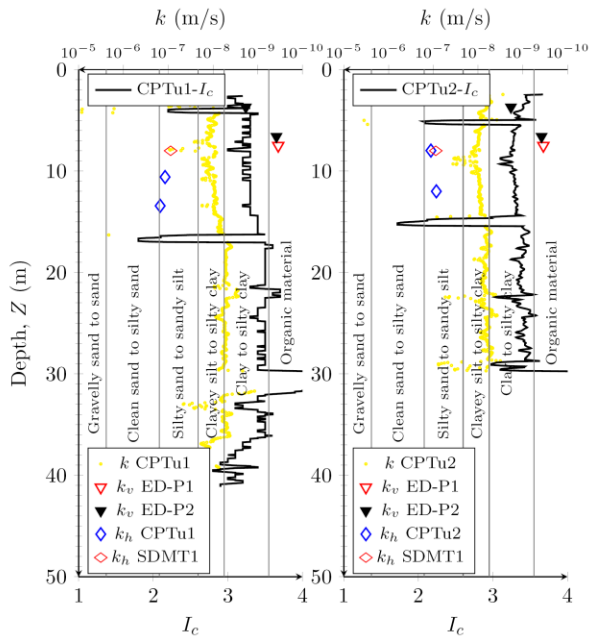
$$K_0=(K_D/ 1.5)^{0.47}-0.6 \quad (12)$$

288 SPT and CPT underestimate K_0 in the upper 15 m depth where DMT evaluates $K_0 \approx 0.8$. This
289 inaccuracy is due to the considerable scatter that exists in the CPT and SPT database used to
290 determine these correlations (Robertson and Cabal, 2015). On the contrary K_0 estimations by all the
291 in situ tests are in reasonable agreement at greater depth providing an average NC value of 0.6
292 between 15 and 30 m depth. This difference between the geotechnical behavior of the upper 15 m-
293 thick layer and the lower 15 m-thick layer, as detected by OCR, K_0 and index parameters (LL, LP,
294 IP, w), may be interpreted as a different concentration of diatoms, higher in the top layer rather than
295 in the bottom one. This assumption is consistent with the analyses of some authors such as Vera-
296 Grunauer (2014), who determined for clays in areas very close to the Murano site that up to 14.5 m
297 depth diatoms are abundant with a density between 5 to 6 million per gram and very well preserved.
298 Moreover, Torres et al. (2018) after studying the temporal variability of diatoms determined that the
299 highest abundance occurs in the first 20 meters.

300 **3.3. Permeability (k)**

301 The vertical coefficient of permeability (k_v) was calculated from the oedometric test, for which the
302 compressibility curve was constructed with the Casagrande methodology and its respective
303 Schmertmann correction (Schmertmann, 1955). In situ tests were also used to determine
304 permeability. Robertson (2010) developed a correlation between the soil behavior type index (I_c)
305 and the coefficient of permeability (k) to obtain an entire but approximate permeability profile that
306 is not sensitive to the anisotropy of the soil. However, better estimation of the horizontal
307 permeability (k_h) can be provided by dissipation tests from both CPTu and DMT. Teh and Houlsby
308 (1991), Perez and Furiel (1988) and Robertson (2010) relationships were used for CPTu tests, once
309 t_{50} , and consequently c_h , were estimated from dissipation curves (Fig. 4). These three correlations

310 provide similar values, and therefore for clarity in Fig. 6 only Robertson (2010) estimation is shown.
 311 Similarly, for DMT test t_{flex} and c_h were used to estimate k_h according to Marchetti and Totani
 312 (1989).



313
 314 **Fig. 7.** Permeability estimates together with soil behaviour index profiles for CPTu1 and CPTu2.

315 The results obtained at Murano site show that all the correlations used to estimate k_h from CPTu
 316 and DMT dissipation tests give very similar interpretations in the soft clays between 8.00 and 13.45
 317 m depth ($k_h \approx 10^{-7}$ m/s), while the continuous k profile derived from I_c only agrees with the
 318 laboratory data in the upper and most permeable clayey layer (≤ 4 m depth). Higher permeability
 319 is encountered in sandy soils ($k \approx 10^{-6}$ m/s) while lower values are confined to soft clay ($k \leq 10^{-9}$
 320 m/s) in reasonable agreement with permeability ranges obtained by Holtz and Kovacs (1981). In
 321 summary, it results indistinct the selection of one permeability correlation in place of another one
 322 as long as a dissipation test is performed, while the “approximation” of k to I_c should only be used
 323 as a guide and option in the absence of dissipation tests, since this methodology can provide results
 324 different for one order of magnitude (or even more), as for the case study of Murano site. Finally,
 325 the results of the dissipation tests are not consistent with the results of the oedometric test even
 326 correcting laboratory- k_v in k_h . According to Tavenas et al. (1983) the permeability measured by
 327 oedometric test regularly gives very low values as a consequence of the hypotheses of Terzaghi's 1-

328 D theory, which considers that the material is isotropic and homogeneous, and therefore it implies
329 the assumption of constant k , M , and c_v during the consolidation.

330 4. Dynamic soil properties at the test site using geotechnical and geophysical measurements

331 4.1. Shear wave velocity

332 The estimation of the shear wave velocity (V_s) is fundamental in geotechnical engineering design,
333 not only for site classification and soil-structure interaction, but also for earthquake analysis and site
334 response. Penetration tests can be used for predicting V_s through some measured parameters. In
335 particular, DMT allows to estimate the small strain shear modulus (G_0), based on the intermediate
336 parameters I_D , K_D , M (Marchetti et al., 2008) and hence V_s , though the theory of elasticity, as follow:

$$V_s = \sqrt{G_0/\rho} \quad (13)$$

337 Where ρ is soil density. The equations to predict G_0 are listed in Table 2:

338 **Table 2.** Equations to estimate V_s from DMT according to Marchetti et al. (2008).

Soil type	G_0 correlation
Silts: $0.6 < I_D < 1.8$	$G_0 = M \cdot 15.686 \cdot K_D^{-0.921}$
Clays: $I_D < 0.6$	$G_0 = M \cdot 26.177 \cdot K_D^{-1.0066}$
Sands: $I_D > 1.8$	$G_0 = M \cdot 4.5613 \cdot K_D^{-0.7967}$

339 Several authors have developed and recommended correlations for SPT, expressed as a function of
340 N_{SPT} , N_{60} , depth (Z), soil type and geological age (Table 3). Finally, for CPT several correlations are
341 available to predict V_s , that are related to numerous parameters like tip resistance (cone tip resistance
342 q_c or corrected cone tip resistance q_t), sleeve friction (f_s), confining stress, depth (Z), soil type, and
343 geologic age (Table 4).

344

345

346

347

348 **Table 3.** Main available equations to estimate V_s from SPT.

349

Author	Soil Type	V_s correlation	Geological description
Wair et al. (2012)	All soils	$V_s = 26 \cdot N_{60}^{0.215} \cdot \sigma'_{v0}{}^{0.275}$	Holocene
	All soils	$V_s = 34 \cdot N_{60}^{0.215} \cdot \sigma'_{v0}{}^{0.275}$	Pleistocene
	Clays and silts	$V_s = 23 \cdot N_{60}^{0.17} \cdot \sigma'_{v0}{}^{0.32}$	Holocene
	Clays and silts	$V_s = 29 \cdot N_{60}^{0.17} \cdot \sigma'_{v0}{}^{0.32}$	Pleistocene
	Sands	$V_s = 27 \cdot N_{60}^{0.23} \cdot \sigma'_{v0}{}^{0.23}$	Holocene
	Sands	$V_s = 35 \cdot N_{60}^{0.23} \cdot \sigma'_{v0}{}^{0.25}$	Pleistocene
Imai and Yoshimura (1970)	All soils	$V_s = 76 \cdot N_{SPT}^{0.33}$	-
Kalteziotis et al. (1992)	All soils	$V_s = 76.2 \cdot N_{SPT}^{0.24}$	-
	Sands and silts	$V_s = 49.1 \cdot N_{SPT}^{0.502}$	
	Clays	$V_s = 76.55 \cdot N_{SPT}^{0.445}$	
Ohsaki and Iwasaki (1973)	All soils	$V_s = 81.4 \cdot N_{SPT}^{0.39}$	-
	Sands	$V_s = 59.4 \cdot N_{SPT}^{0.47}$	
Iyisan (1996)	All soils	$V_s = 51.5 \cdot N_{SPT}^{0.516}$	Deep alluvial deposits
Jinan (1987)	All soils	$V_s = 116.10 \cdot (N_{SPT} + 0.32)^{0.202}$	Soft Holocene deposits
Dikmen (2009)	All soils	$V_s = 58 \cdot N_{SPT}^{0.39}$	Quaternary alluvium
	Sands	$V_s = 73 \cdot N_{SPT}^{0.33}$	Quaternary alluvium
	Clays	$V_s = 44 \cdot N_{SPT}^{0.48}$	Quaternary alluvium
	Silt	$V_s = 60 \cdot N_{SPT}^{0.36}$	Quaternary alluvium

350

351 **Table 4.** Main available equations to estimate V_s from CPT.

352

Author	V_s (or G_0) correlation	Geological description
Robertson (2012)	$V_s = \alpha_{vs} \cdot (q_t - \sigma'_{v0})^{0.5} / p_a$; $\alpha_{vs} = 10^{0.55 \cdot I_c + 1.68}$	Holocene and Pleistocene soils, mostly uncemented
Hegazy and Mayne (1995)	$V_s = [10.1 \log(q_t) - 11.4]^{1.67} \cdot f_s / q_t \cdot 100$	All types of soils
Simonini and Cola (2000)	$G_0 = 49.2 \cdot q_c^{0.51}$	Sand, silt and silty clay of Venice Lagoon
Andrus et al. (2007)	$V_s = 2.27 \cdot q_t^{0.412} \cdot I_c^{0.989} \cdot Z^{0.033} \cdot ASF$; ASF = 1.00	Holocene soils
	$V_s = 2.62 \cdot q_t^{0.395} \cdot I_c^{0.912} \cdot Z^{0.124} \cdot SF$; SF = 1.12	Pleistocene soils
Madiari and Simoni (2004)	$V_s = 140 \cdot q_c^{0.30} \cdot f_s^{-0.13}$	Holocene cohesive soils
	$V_s = 268 \cdot q_c^{0.21} \cdot f_s^{0.02}$	Holocene incoherent soils
	$V_s = 182 \cdot q_c^{0.33} \cdot f_s^{-0.02}$	Pleistocene cohesive soils
	$V_s = 172 \cdot q_c^{0.35} \cdot f_s^{-0.05}$	Pleistocene incoherent soils
Bouchovalas et al. (1989)	$G_0 = 28.0 \cdot q_c^{1.40}$	Very soft clays
Vera-Grunauer (2014)	$V_s = \sqrt{\eta \cdot q_c \cdot e^\alpha}$; $\alpha = [(3N_{kc} - 4) / 4] - [1 / (2\beta)]$; $\eta = 3g / [2N_{kc} \cdot \gamma_s \cdot (1 + \nu)]$	Clays with diatoms

353

354 p_a = atmospheric pressure; ASF = Age scaling factor; SF = Scaling factor; γ_s = volumetric weight; g = gravity;

355 N_{kc} = correlation factor; β = ratio between undrained shear strength and effective vertical stress; ν = Poisson's constant.

356 Fig. 8a provides the comparison between V_s measured and V_s predicted by DMT, that shows a

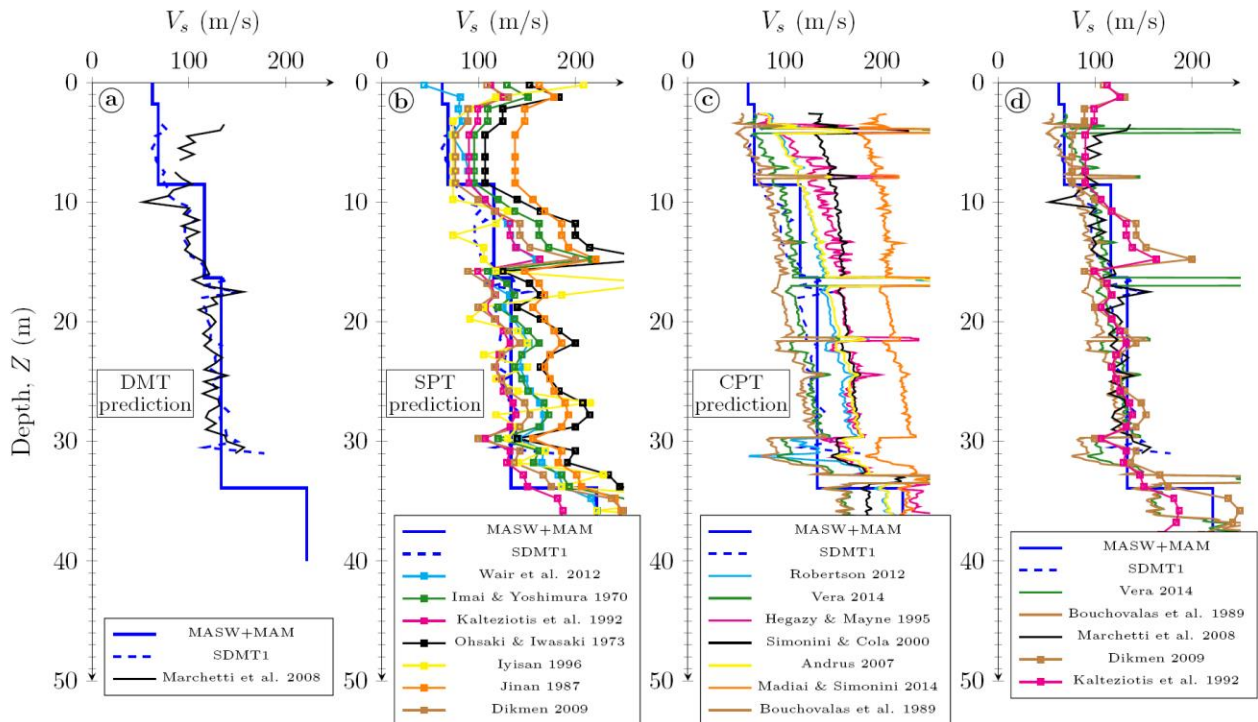
357 reasonable agreement. There is a slight overestimation of DMT values, more pronounced in the

358 upper 15 m that could be related to the higher concentration of the diatoms as previously detected

359 by K_D (through K_0 and OCR) that is noticeable more reactive to stress history, structure and

prestraining/aging, scarcely felt by q_c (or q_t) from CPT (Amoroso, 2014). A large number of

360 correlations have been developed for SPT, involving the soil type, the geological description, and
 361 sometimes the in situ stress. This results in a wide variability (Fig. 8b) within the V_s profiles, as
 362 previously noted also by other authors in other sites (e.g. Fabbrocino et al. 2015, Akin et al., 2011),
 363 and confirmed for the soft clay deposits of Murano test site (Fig. 8c) (e.g. Jinan, 1987 estimates
 364 values up to two times the measured ones).



365 **Fig. 8.** Comparison of V_s measured and V_s predicted by DMT (a), SPT (b), and CPTu (c);
 366 comparison of V_s measured and V_s predicted using the best correlations. The plots correspond to
 367 borehole P1, CPTu1 and SDMT1 tests.
 368
 369 A similar behaviour (Fig. 8c) is observed with the V_s correlations developed for CPT test (e.g.
 370 Robertson, 2012 estimates values up to four times the measured ones). The arisen uncertainty could
 371 be due to the dependency to numerous and different parameters mentioned above that CPT and SPT
 372 parameters may not capture correctly. However, it is possible to select the best SPT- V_s and CPT- V_s
 373 predictions for soft clay deposits using the formulas proposed by Wair et al. (2012), Dikmen (2009)
 374 and Kalteziotis et al. (1992) for SPT test. Interestingly, the last two equations developed for all types
 375 of soils are in better agreement with the measured V_s profile than those made exclusively for clays.
 376 The selected Wair et al. (2012) equation is valid for Holocene clays and silts. For CPT test,

377 Bouchovalas et al. (1989) and Vera-Grunauer (2014) resulted to fit better with V_s measurements,
 378 and they are valid for very soft clays and for clays with diatoms (Fig. 8c). In particular, Vera-
 379 Grunauer (2014) proposed a site-specific correlation calibrated using Guayaquil dataset, that for D3
 380 zone it established the following input parameters: $\beta=0.22$; $N_{kc}=12$; $\gamma_s=15$ KN/m³; $\nu=0.3$. All
 381 together the measured (SDMT, MASW+MAM) and selected-predicted (Marchetti et al., 2008; Wair
 382 et al., 2012; Dikmen, 2009; Kalteziotis et al., 1992; Bouchovalas et al., 1989; Vera-Grunauer, 2014)
 383 V_s data presented reasonable agreement identifying V_s values increasing in the 30 m depth in range
 384 of 50-180 m/s.

385 4.2. Stiffness decay curves

386 Finally, in situ tests were used to evaluate stiffness decay curves (G - γ curves). In particular, this
 387 opportunity is offered by the seismic dilatometer that allows to estimate the in situ variation of soil
 388 stiffness with the level of deformation, as preliminarily suggested by Marchetti et al. (2008) and
 389 then tested by Amoroso et al. (2014) and Di Mariano et al. (2019). The method proposes firstly to
 390 assess the small strain modulus G_0 though the theory of elasticity using V_s (Eq. 13).

391 Then it is necessary to evaluate a working strain shear modulus G_{DMT} starting from the constrained
 392 modulus (M also named M_{DMT}) obtained from the usual DMT test though the theory of elasticity:

$$G_{DMT} = M_{DMT} \cdot (1-2\nu) / [2 \cdot (1-\nu)] \quad (14)$$

393 where ν = Poisson's ratio, assumed equal to 0.3 for all layers.

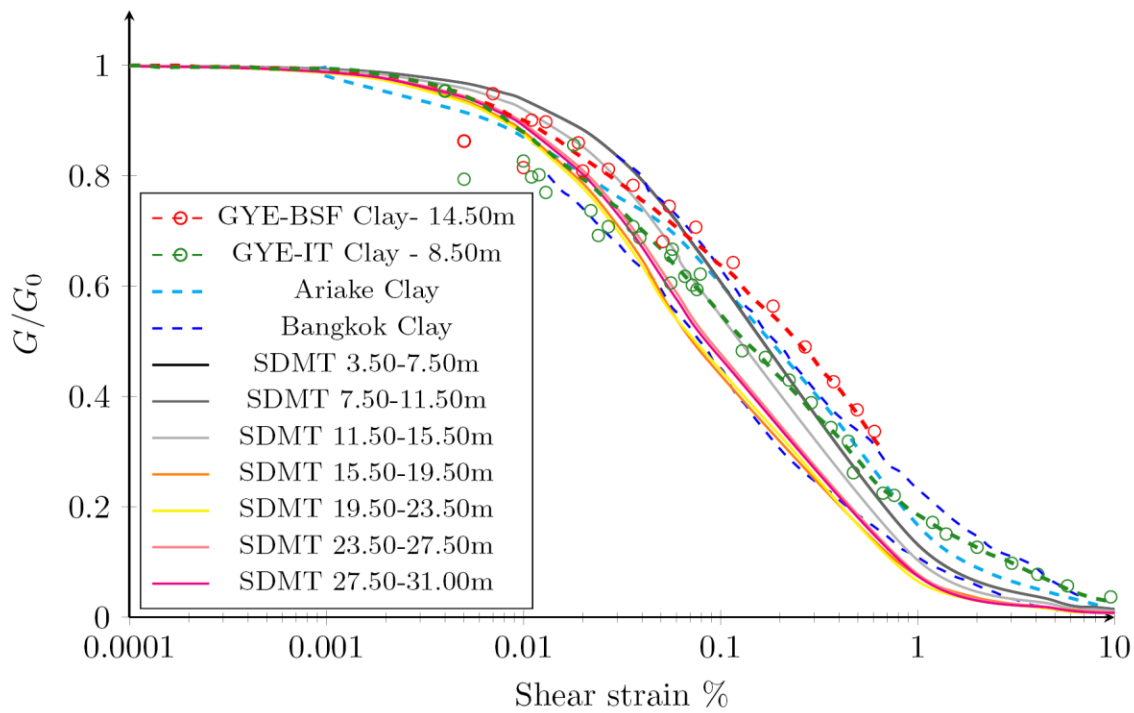
394 Amoroso et al. (2014) proposed an equation to determine a hyperbolic stress-strain equation to
 395 represent the non-linear soil behavior through a normalized decay curve (G/G_0 - γ curve) by SDMT
 396 data:

$$G/G_0 = 1 / [1 + (G/G_{DMT} - 1) \cdot (\gamma/\gamma_{DMT})] \quad (15)$$

397 where G = shear modulus; γ = shear strain; γ_{DMT} = shear strain associated with the working strain
 398 DMT modulus for which Amoroso et al. (2014) suggested range of values based on the soil type.

399 In this particular case, being Murano site composed by soft clays, it is recommendable to use a value
 400 of $\gamma_{DMT} = 2\%$. Moreover, to consider the effect of the confining stress and the different geotechnical

401 properties of the entire soil profile into the assessment of the G/G_0 - γ curves, seven homogeneous
 402 strata were identified from 3.50 to 31 m depth. The average values used to construct the non linear
 403 curves plotted in Fig. 9 are reported in Table 5. The G/G_0 - γ curves estimated in the upper 15.5 m
 404 have a similar behavior, while the deeper G/G_0 - γ curves decay much faster. This aspect is related to
 405 the higher values of K_D , and hence of OCR and K_0 , detected for the upper layer, confirming a
 406 possible relationship with the different concentration of the diatoms.



407
 408 **Fig. 9.** G - γ decay curves for Guayaquil clays obtained by SDMT tests and comparison with results
 409 of laboratory curves.

410 **Table 5.** Average values used to construct G/G_0 - γ curves.

Depth	Soil type	G_0 (MPa)	M_{DMT} (MPa)	ν	G_{DMT} (MPa)	G_{DMT}/G_0	γ_{DMT} (%)
3.50-7.50	Soft clay	7.22	1.79	0.30	0.51	0.07	2
7.50-11.50	Soft clay	11.45	2.82	0.30	0.81	0.07	2
11.50-15.50	Soft clay	17.21	3.30	0.30	0.94	0.05	2
15.50-19.50	Soft clay	26.40	3.29	0.30	0.94	0.04	2
19.50-23.50	Soft clay	26.22	3.12	0.30	0.89	0.03	2
23.50-27.50	Soft clay	28.85	4.14	0.30	1.18	0.04	2
27.50-31.00	Soft clay	32.41	4.44	0.30	1.27	0.04	2

411 Fig. 9 also plots two G/G_0 - γ curves developed for Guayaquil clays in geological zone D3A whose
 412 samples were retrieved at Baseball Stadium Field (BSF-dashed red line) on OC clays and at

413 Trinitaria Island (TI-dashed green line) on NC clays according to Vera-Grunauer (2014). The cyclic
414 response of TI samples was evaluated by means of cyclic triaxial and simple shear tests while, for
415 BSF clay, the decay curve was estimated from cyclic triaxial data. The conditions of the clay
416 structure were modelled in the following way: to reproduce the conditions of the OC clay, the
417 recompression method was used during the consolidation stage and the SHANSEP procedure was
418 applied to model the normally consolidated soil. As reported by Vera-Grunauer (2014), the lower
419 decay of BSF clay is due to the influence of pyrite cementation in its soil fabric. Other laboratory
420 curves are included in Fig. 9 for naturally cemented alluvial clays with diatoms: Bangkok clay
421 (Teachavoransinskun et al., 2002) and Ariake clay (Nagase et al., 2006).

422 A reasonable agreement is possible to detect by comparing the entire group of literature curves with
423 $G/G_0-\gamma$ curves by SDMT. However, the best fitting can be found between Guayaquil and Bangkok
424 (upper limit) laboratory tests and SDMT prediction within the upper 15.5 m, probably due to the
425 higher content of diatoms. Below that depth, SDMT assessment fits well with the lower limit of
426 Bangkok clays.

427 **5. Conclusions**

428 The deep site campaign performed in Guayaquil (Ecuador) at the Murano site allowed to provide a
429 better soil characterization for soft clays in presence of diatoms. In particular, the soil deposits were
430 classified both using physical characteristics (i.e. USCS) and in situ tests (i.e. CPTu and DMT). In
431 particular, index properties looked to be influenced by the diatom content. In this respect, the
432 microstructure and porous shape of diatoms increased the average PI and w values in the upper 15
433 m depth, influencing the interpretation provided by USCS classification. This aspect is less visible
434 from I_c and I_D , while it resulted well detected by in situ soil stiffness and strength.

435 In general terms, the parameters of resistance, compressibility and stress history provided reliable
436 values using both CPT and DMT, while SPT and laboratory tests usually detected lower values.
437 SPT test is not particularly effective for soft soil, while characterization of soil behavior by
438 laboratory tests is directly dependent on the sampling process. Soft soil sampling procedure can

439 modify the soil structure, and therefore soil behavior from laboratory differs considerably from the
440 corresponding in situ behavior. The analysis especially of the OCR profiles by CPTu and DMT
441 confirmed the presence of diatoms in the upper 15 m ($OCR \approx 2$) and their lower concentration below
442 this depth ($OCR \approx 1$). Similar observations emerged from K_0 values obtained only by DMT: K_0
443 decreases from 0.8 to 0.6 moving from the upper 15 m to the lower layer. The better K_0 prediction
444 by DMT is related to the intermediate range of strain to which the test is associated (Baligh and
445 Scott, 1975; Mayne, 2001), and consequently to the direct correlation between K_0 and K_D ,
446 considering K_D a stress history indicator and an amplified K_0 . The above findings are in agreement
447 with Vera-Grunauer (2014) and Torres et al. (2018) who identified soft clays with diatoms in the
448 upper 15-20 m in Guayaquil bay.

449 Due to the porous shape of diatoms, a considerable increase in permeability would have been
450 expected in the upper layer. However, in situ and laboratory measurements are not available along
451 the entire profile, but only in the upper 15 m depth. According to the results obtained, it is evident
452 that CPTu and DMT dissipation tests gave very similar results for this type of clays.

453 On the contrary, parameters obtained from the oedometric tests lead to inconsistent results, probably
454 because of sample disturbance and due to the assumptions made to interpret the permeability
455 through the 1D Terzaghi's theory, which do not properly fit the behavior of natural clays (Tavenas
456 et al. 1983). The comparison between predicted and measured V_s values suggested that DMT
457 prediction is more reliable than CPT and SPT predictions. The high number of V_s correlations
458 developed for CPT and SPT test detected a wide variability within the V_s profile of the soft clays,
459 resulting in contrast with the single equation available for DMT (Marchetti et al., 2008). The arisen
460 uncertainty could be due to the dependency to numerous and different parameters related to the
461 geological age, soil type and in situ stress state that CPT and SPT parameters may not capture
462 correctly. At the same time, DMT (through K_D) is well correlated to stress history,
463 prestraining/aging and structure scarcely felt by q_c and N_{SPT} (Amoroso, 2014).

464 Finally, the nonlinear soil behavior of the soft clays at Murano site was presented by means of
465 literature data and direct SDMT data interpretation. The G/G_0 - γ decay curves in the estuarine deltaic
466 clays (zone D3) resulted in good agreement using SDMT and cyclic triaxial tests, identifying a
467 similar behavior in the curves of upper 15.5 m, while the deeper G/G_0 - γ curves decay much faster.
468 This aspect resulted related to the higher values of K_D , and hence of OCR and K_0 , detected for the
469 upper layer, confirming a possible relationship with the different concentration of the diatoms. The
470 use of SDMT in estimating stiffness decay curves could be therefore advantageous for the
471 geotechnical design, although further investigation is needed to better understand the influence of
472 diatoms content on decay curves.

473 **Acknowledgements**

474 Special thanks to Studio Prof. Marchetti (Italy) for kindly providing the SDMT apparatus and to
475 Prof. Maurizio Mulas (Escuela Superior Politécnica del Litoral, Ecuador) for sharing scientific
476 geological information of the studied area.

477 **Declaration of competing interest**

478 The authors declare that they have no known competing financial interests or personal relationships
479 that could have appeared to influence the work reported in this paper.

480 **References**

- 481 Akin, M.K., Kramer, S.L., Topal, T., 2011. Empirical correlations of shear wave velocity (V_s) and
482 penetration resistance (SPT-N) for different soils in an earthquake-prone area (Erbaa-
483 Turkey). *Eng. Geol.* 119, 1–17. <https://doi.org/10.1016/j.enggeo.2011.01.007>.
- 484 Amoroso, S., 2014. Prediction of the shear wave velocity V_s from CPT and DMT at research sites.
485 *Front. Struct. Civ. Eng.* 8, 83–92. <https://doi.org/10.1007/s11709-013-0234-6>.
- 486 Amoroso, S., Monaco, P., Lehane, B., Marchetti, D., 2014. Examination of the potential of the
487 seismic dilatometer (SDMT) to estimate in situ stiffness decay curves in various soil types.
488 *Soils and Rocks.* 37, 177–194.

489 Andrus, R.D., Mohanan, N.P., Piratheepan, P., Ellis, B.S., Holzer, T.L., 2007. Predicting shear-
490 wave velocity from cone penetration resistance, in: Proc. of the 4th International
491 Conference on Earthquake Geotechnical Engineering. Thessaloniki, Greece.

492 Antonides, L. 1998. Diatomite, in: Minerals Year Book. United States Geological Survey, Reston,
493 Virginia, pp. 56–57.

494 ASTM, D., 2011. 2487, Standard Classification of Soils for Engineering Purposes (Unified Soil
495 Classification System). Annual Book of ASTM Standards. 4, 206–215.

496 Baligh, M.M., Scott, R.F., 1975. Quasi-static deep penetration in clays. J. Geotech. Geoenviron.
497 Eng. 101,1119-1133.

498 Benítez, S., Álvarez, V., Vera-Grunauer, X., Mera, W., 2005. Geological study of Guayaquil city,
499 in: Special Report. UCSG, Guayaquil.

500 Benitez, S.B., 1995. Geodynamic evolution of the south Ecuadorian coastal province in the upper
501 tertiary cretaceous. *Géologie Alpine*. 71, 3-163 (in French).

502 Berisavljević, D., Berisavljević, Z., Čebašek, V., Šušić, N., 2014. Characterisation of collapsing
503 loess by seismic dilatometer. *Eng. Geol.* 181, 180–189.
504 <https://doi.org/10.1016/j.enggeo.2014.07.011>.

505 Berisavljević, D., 2017. Geotechnical soil modeling based on the parameters obtained by seismic,
506 PhD thesis. University of Belgrade, Serbia.

507 Boncio, P., Amoroso, S., Galadini, F., Galderisi, A., Iezzi, G., Liberi, F. 2020. Earthquake-induced
508 liquefaction features in a late quaternary fine-grained lacustrine succession (Fucino Lake,
509 Italy): implications for microzonation studies. *Eng. Geol.* 272, 105621,
510 <https://doi.org/10.1016/j.enggeo.2020.105621>.

511 Bouckovalas G., Kalteziotis N., Sabatakakis N., Z.H., 1989. Shear wave velocity in a very soft clay-
512 measurements and correlations., in: Taylor & Francis (Eds.), Proc. of the 12th International
513 Conference Soil Mechanics Foundation Engineering (ICSMFE). Rio de Janeiro, Brazil, pp.
514 191–194.

515 Brown, T., Hettiarachchi, H., 2008. Estimating shear strength properties of soils using SPT blow
516 counts: an energy balance approach, in: Alshawabkeh, A. N., Reddy, K.R., Khire, M.V.
517 (Eds.), *GeoCongress 2008: Characterization, Monitoring, and Modeling of GeoSystems*.
518 New Orleans, Louisiana, pp. 364–371. [https://doi.org/10.1061/40972\(311\)46](https://doi.org/10.1061/40972(311)46)

519 Caicedo, B., Mendoza, C., López, F., Lizcano, A., 2018. Behavior of diatomaceous soil in lacustrine
520 deposits of Bogotá, Colombia. *J. Rock Mech. Geotech. Eng.* 10, 367–379.
521 <https://doi.org/10.1016/j.jrmge.2017.10.005>

522 Chunga, K., Ochoa-Cornejo, F., Mulas, M., Toulkeridis, T., Menéndez, E. 2019). Characterization
523 of geological faults related to cortical earthquakes of Guayaquil Gulf (Ecuador). *Andean
524 geology*, 46(1), 66-81 (in Spanish).

525 Chunga, K., Quiñonez Macías, M., 2005. Seismic hazard assessment for Guayaquil city (Ecuador):
526 insights from quaternary geological data. *Geológica del Perú*. 32, 225-238.

527 Devincenzi, M., Powell, J.J.M., Cruz, N., De Toledo, M.A.Á., 2007. Present use of geotechnical in
528 situ tests. *Revista Digital del Cedex*. 31 (in Spanish).

529 Di Mariano, A., Amoroso, S., Arroyo, M., Monaco, P., Gens, A., 2019. SDMT-based numerical
530 analyses of deep excavation in soft soil. *J. Geotech. Geoenviron. Eng.* 145, 04018102.
531 [https://doi.org/10.1061/\(asce\)gt.1943-5606.0001993](https://doi.org/10.1061/(asce)gt.1943-5606.0001993)

532 Díaz Rodríguez, J.A., González Rodríguez, R.R., 2013. Influence of diatom microfossils on soil
533 compressibility, in: Delage, P., Desrues, J., Frank, R., Puech, A., Schlooser, F. (Eds.), *Proc.
534 of the International XVIII Conference on Soil Mechanics and Geotechnical
535 Engineering*. Presses des Ponts, Paris, France, pp. 325-328.

536 Dikmen, Ü., 2009. Statistical correlations of shear wave velocity and penetration resistance for soils.
537 *Journal of Geophysics and Engineering*. 6, 61–72.

538 Egüez A., Alvarado, A., Yepes, H., Machette, M.N., Costa, C.H., Dart, R.L., Bradley, L.A., 2003.
539 Database and map of Quaternary faults and folds of Ecuador and its offshore regions. US
540 Geological Survey Open-File Report. 3, 289.

541 Fabbrocino, S., Lanzano, G., Forte, G., de Magistris, F.S., Fabbrocino, G., 2015. SPT blow count
542 Vs. shear wave velocity relationship in the structurally complex formations of the Molise
543 Region (Italy). Eng. Geol. 187, 84–97.

544 Hegazy, Ya., Mayne, P.W., 1995. Statistical correlations between Vs and cone penetration data for
545 different soil types, in: Proc. of the International Symposium on Cone Penetration Testing,
546 CPT. Linköping, Sweden, pp. 173–178.

547 Holtz, R.D., Kovacs, W.D., Sheahan, T.C., 1981. An Introduction to Geotechnical Engineering,
548 second ed. Prentice Hall, Englewood Cliffs.

549 Imai, T., Yoshimura, Y., 1970. Elastic wave velocity and soil properties in soft soil. Tsuchi-to-
550 Kiso. 18, 17–22 (in Japanese).

551 Iyisan, R., 1996. Correlations between shear wave velocity and in-situ penetration test results.
552 Teknik Dergi. 7, 371–374 (in Turkish).

553 Jamiolkowski, M., Ghionna, V.N., Lancellotta, R., Pasqualini, E., 1988. New correlations of
554 penetration tests for design practice, in: Proc. International Symposium on penetration
555 testing; ISOPT-1. A.A. Balkema Publishers, Rotterdam, pp. 263–296.

556 Jinan, Z., 1987. Correlation between seismic wave velocity and the number of blow of SPT and
557 depth. Chin. J. Geotech. Eng. 92–100.

558 Kalteziotis, N., Sabatakakis, N., Vassiliou, J., 1992. Evaluation of dynamic characteristics of Greek
559 soil formations, in: Second Hellenic Conference on Geotechnical Engineering. pp. 239–
560 246 (in Greek).

561 Kulhawy, F.H., Mayne, P.W., 1990. Manual on Estimating Soil Properties for Foundation Design.
562 Electric Power Research Inst., Palo Alto, CA (USA).

563 Look, B.G., 2007. Handbook of Geotechnical Investigation and Design Tables, second edition. CRC
564 Press/Balkema, EH Leiden, The Netherlands.

565 Losic, D., Pillar, R. J., Dilger, T., Mitchell, J. G., Voelcker, N.H., 2007. Atomic force microscopy
566 (AFM) characterization of the porous silica nanostructure of two centric diatoms. *J. Porous*
567 *Mater.* 14, 61–69.

568 Madiai, C., Simoni, G., 2004. Shear wave velocity-penetration resistance correlation for Holocene
569 and Pleistocene soils of an area in central Italy, in: Proc., 2nd International Conference
570 on Geotechnical Site Characterization (ISC'2), Porto, Portugal, pp.1687–1694.

571 Marchetti, S., Crapps, D.K., 1981. Flat Dilatometer Manual. Schmertmann and Crapps Inc.,
572 Gainesville.

573 Marchetti, S., 1980. In situ tests by flat dilatometer. *J. Geotech. Eng. Div.* 106, 299–321.

574 Marchetti, S., Monaco, P., Totani, G., Calabrese, M., 2001. The flat dilatometer test (DMT) in soil
575 investigations: a report by the ISSMGE committee TC16, in: Proc. 2nd International Flat
576 Dilatometer Conference. American Society of Civil Engineers. Reston, VA, pp. 7-48.

577 Marchetti, S., Monaco, P., Totani, G., Marchetti, D., 2008. In situ tests by seismic dilatometer
578 (SDMT), in: Proc. of the From Research to Practice in Geotechnical Engineering. ASCE
579 *Geotech*, pp. 292–311. [https://doi.org/10.1061/40962\(325\)7](https://doi.org/10.1061/40962(325)7)

580 Marchetti, S., Totani, G., 1989. Ch evaluation from DMTA dissipation curves, in: Proc. 12th
581 International Conference on Soil Mechanics and Foundation Engineering. A.A. Balkema
582 Publishers, Rio de Janeiro, pp. 281–286.

583 Mayne, P., 2006. In-Situ Test Calibrations for Evaluating Soil Parameters, in: Taylor & Francis
584 (Eds.), Characterisation and Engineering Properties of Natural Soils—Proc. of the 2nd
585 International Workshop on Characterisation and Engineering Properties of Natural Soils.
586 pp. 1601-1652.

587 Mayne, P.W., 2016. Evaluating effective stress parameters and undrained shear strengths of soft-
588 firm clays from CPT and DMT. *Aust. Géoméch. J.* 51, 27–55.

589 Mayne, P.W., 2006. Interrelationships of DMT and CPT readings in soft clays, in: R.A. Failmezger
590 and J. B. Anderson (Eds.), Proc. 2nd International Conference on Flat
591 Dilatometer. Washington, D.C., pp. 231-236.

592 Mayne, P.W., 2005. Unexpected but foreseeable mat settlements on Piedmont residuum. ISSMGE
593 International Journal of Geoenvironmental Engineering Case Histories. 1, 5–17.

594 Mayne, P.W., 2001. Stress-strain-strength-flow parameters from enhanced in-situ tests, in: Proc.
595 Int. Conf. on In Situ Measurement of Soil Properties and Case Histories. Bali, pp. 27–47.

596 Mayne, P.W., Coop, M.R., Springman, S., Huang, A.-B., Zornberg, J., 2009. SOA-1: Geomaterial
597 behavior and testing, in: Proc. 17th International Conference on Soil Mechanics and
598 Geotechnical Engineering. Millpress, Rotterdam, The Netherlands, pp. 2777–2872.

599 Mayne, P.W., Liao, T., 2004. CPT-DMT interrelationships in Piedmont residuum. in: Proc. 2nd
600 International Conference on Geotechnical Site Characterization (ISC'2), Porto, Portugal,
601 pp. 345–350.

602 Monaco, P., Amoroso, S., Marchetti, S., Marchetti, D., Totani, G., Cola, S., Simonini, P., 2014.
603 Overconsolidation and stiffness of Venice lagoon sands and silts from SDMT and CPTU.
604 J. Geotech. Geoenviron. Eng. 140, 215–227. [https://doi.org/10.1061/\(ASCE\)GT.1943-](https://doi.org/10.1061/(ASCE)GT.1943-5606.0000965)
605 [5606.0000965](https://doi.org/10.1061/(ASCE)GT.1943-5606.0000965).

606 Monaco, P., Calabrese, M., 2006, DMT-Predicted Vs. Observed Settlements: A Review of the
607 Available Experience, in: R. A. Failmezger and J. B. Anderson (Eds.), Proc. 2nd
608 International Conference on Flat Dilatometer. Washington, D.C., pp. 244–252.

609 Nagase, H., Shimizu, K., Hiro-Oka, A., Tanoue, Y., Saitoh, Y., 2006. Earthquake-induced residual
610 deformation of Ariake clay deposits with leaching. Soil Dyn. Earthq. Eng. 26, 209–220.

611 Ohsaki, Y., Iwasaki, R., 1973. On dynamic shear moduli and Poisson's ratios of soil deposits. Soils
612 Found. 13, 61–73.

613 Parez, L., Fauriel, R., 1988. The piezocone improvements made to soil recognition. Revue française
614 de géotechnique. 13–27 (in French).

615 Park, C.B., Miller, R.D., Xia, J., Ivanov, J., 2007. Multichannel analysis of surface waves (MASW)-
616 active and passive methods. *Lead. Edge.* 26, 60–64.

617 Robertson, P.K., 2012. Discussion of Influence of particle size on the correlation between shear
618 wave velocity and cone tip resistance. *Can. Geotech. J.* 49, 121–123.

619 Robertson, P.K., 2010. Estimating in-situ soil permeability from CPT & CPTu, in: *Memorias Del*
620 *2nd International Symposium on Cone Penetration Testing.* California State Polytechnic
621 University, Pomona, CA.

622 Robertson, P.K., 2009. Interpretation of cone penetration tests-a unified approach. *Can. Geotech. J.*
623 46, 1337–1355.

624 Robertson, P.K., Cabal, K.L., 2015. *Guide to Cone Penetration Testing for Geotechnical*
625 *Engineering,* sixth ed. Gregg Drilling and Testing Inc., Signal Hill.

626 Robertson, P.K., Sully, J.P., Woeller, D.J., Lunne, T., Powell, J.J.M., Gillespie, D.G., 1992.
627 Estimating coefficient of consolidation from piezocone tests. *Can. Geotech. J.* 29, 539–
628 550. <https://doi.org/10.1139/t92-061>

629 Rodríguez, J.F., Auvinet, G., Martínez, H.E., 2015. Settlement analysis of friction piles in
630 consolidating soft soils. *DYNA. Journal of facultad de minas, Universidad Nacional de*
631 *Colombia.* 82, 211–220. <https://doi.org/http://dx.doi.org/10.15446/dyna.v82n192.47752>.

632 Schmertmann, J.H., 1988. Dilatometers settle in. *Civil Engineering.* 58, 68.

633 Schmertmann, J.H., 1986. Dilatometer to compute foundation settlement, in: *Proc. In Situ.*
634 *Schmertmann & Crapps Inc., Gainesville, FL,* pp. 303–321.

635 Schmertmann, J.H., 1955. The undisturbed consolidation behaviour of clay. *Trans.* 120, 1201–1233.

636 Shiwakoti, D.R., Tanaka, H., Tanaka, M., Locat, J., 2002. Influences of diatom microfossils on
637 engineering properties of soils. *Soils Found.* 42, 1–17.

638 Simonini, P., Cola, S., 2000. Use of piezocone to predict maximum stiffness of Venetian soils. *J.*
639 *Geotech. Geoenviron. Eng.* 126, 378–382.

640 Tavenas, F., Leblond, P., Jean, P., Leroueil, S., 1983. The permeability of natural soft clays. Part I:
641 Methods of laboratory measurement. *Can. Geotech. J.* 20, 629–644.

642 Teachavorasinskun, S., Thongchim, P., Lukkunaprasit, P., 2002. Shear modulus and damping of
643 soft Bangkok clays. *Can. Geotech. J.* 39, 1201–1208.

644 Teh, C.I., Houlsby, G.T., 1991. An analytical study of the cone penetration test in clay.
645 *Géotechnique.* 41, 17–34. <https://doi.org/10.1680/geot.1991.41.1.17>

646 Torres, G., Recalde, S., Narea, R., Troccoli, L., Rentería, W., 2018. Spatio-temporal variability of
647 phytoplankton and oceanographic variables in El Golfo de Guayaquil during 2013-15. *J.*
648 *Dep. Eng. FIGMMG-UNMDM.* 20, 70–79 (in Spanish).

649 Treguer, P., Nelson, D.M., van Bennekom, A.J., DeMaster, D.J., Leynaert, A., Queguiner, B., 1995.
650 The silica balance in the world ocean: a reestimate. *Science.* 268, 375–379.

651 Vera-Grunauer, X., 2014. Seismic response of a soft, high plasticity, diatomaceous naturally
652 cemented clay deposit, PhD thesis. University of California, Berkeley.

653 Wair, B.R., DeJong, J.T., Shantz, T., 2012. Guidelines for Estimation of Shear Wave Velocity
654 Profiles, in: Report 2012/08. Pacific Earthquake Engineering Research Center, California,
655 USA.

656 Yu, H.-S., 2004. James K. Mitchell Lecture. In situ soil testing: from mechanics to interpretation, in:
657 Proc., 2nd International Conference on Geotechnical Site Characterization (ISC'2), Porto,
658 Portugal, pp. 3–38.

659